



# Assessment of mechanical properties in high-strength steel weld metals by means of phase transformation temperature

Rahul Sharma<sup>1</sup> · Uwe Reisgen<sup>1</sup>

Received: 21 October 2017 / Accepted: 9 May 2018 / Published online: 19 May 2018  
© International Institute of Welding 2018

## Abstract

The evaluation of the mechanical properties of weld metals in structural steels is one of the most important factors of weld quality control. Improvements in methods of tensile strength assessment could facilitate the choice and development of suitable filler materials. For low-alloyed ferritic steel weld metals, the mechanical properties depend strongly on the cooling rate of the weld. Since the formation of ferrite and bainite is diffusion controlled, the solid state phase transformation temperatures are also influenced by the cooling rate. In this paper, experimental analyses of the mechanical properties of welded joints in high-strength structural steels are made taking into account the phase transformation temperature of the weld metal. Therefore, joint welds of quenched and tempered and TMCP high-strength structural steels in the yield strength range between 690 and 1100 MPa were carried out using the gas metal arc welding process. Within the welding setup a pyrometer was used to acquire the cooling curve of the weld metal surface. This allowed to apply the single-sensor DTA method for the determination of phase transformation temperatures. A comparison with longitudinal tensile test results showed that a correlation between tensile strength and phase transformation start temperature exists for the welded joints under investigation. Even for yield strength and notch impact toughness, a relationship could be observed. For a reduced phase transformation temperature, higher yield strength and impact toughness were found.

**Keywords** Strength · Transformation · Low alloy steels · QT steels · Weld metal

## 1 Introduction

High-strength weld metals are a key factor for the production of resource efficient welded components. For many applications, structural steels with a yield strength level from 690 to 960 MPa are common today. Special applications, such as mobile crane construction, also benefit from steel grades which deliver yield strength levels of up to 1300 MPa due to their martensitic microstructure.

Besides the good results concerning the usability properties of these steels, the availability of matching welding filler metals of the same strength level is currently not given.

According to standard classification, the welding wire available on the market for gas metal arc welding which forms the strongest weld metal is EN ISO 16834-A G Mn4Ni2.5CrMo (AWS A5.28 ER120S-G) [1, 2]. Weld metals of increased strength level would provide even more possibilities for resource efficient manufacturing of welded components through reduction of wall thickness and weight reduction. The mechanical properties of steel weld metals depend mainly on features such as chemical composition, thermal cycle and non-metallic inclusion size and distribution, solidification structure, and prior austenite grain size which altogether influence the microstructure of a weld [3].

For the relationship between welding parameters and mechanical properties in low-alloyed steels, the cooling time is considered as a major criterion, as it strongly affects the resulting microstructure and thus, the mechanical properties [4]. Furthermore, empirical formulas for the calculation of cooling times from the basic welding parameters (Heat input, plate thickness) lead to good results for many applications [5, 6]. Besides the ease of use for weld quality assurance and production planning purposes, there is no explicit

---

Recommended for publication by Commission IX - Behaviour of Metals Subjected to Welding

---

✉ Rahul Sharma  
sharma@isf.rwth-aachen.de

<sup>1</sup> Welding and Joining Institute, RWTH Aachen University, Pontstr. 49, 52062 Aachen, Germany

relationship between cooling times and mechanical properties, applying to more than a specific chemical composition. Therefore, a specific function is needed to express the relationship between cooling time and the regarded mechanical property. This information can be taken from a continuous cooling transformation (CCT) diagram, given that it contains hardness values. Since the effort to determine CCT diagrams through dilatometric measurements is high, time consuming, and not always possible at all, alternative methods such as numerical modeling of material properties or statistically based surrogate modeling also enable to estimate the mechanical properties.

In order to find proper relationships between chemical composition, welding process conditions, and resulting properties, extensive data analyses have been carried out using neural network methods [7, 8], but the specific impact of the thermal cycle was not within the objective of the research. However, the found models can help to determine suitable ranges for the chemical composition of weld metals for a given mechanical property level. Experimentally determined phase transformation data for ferritic steel weld metals within the welding thermal cycle have been reported, among others, in [9–11]. A more sophisticated way is the use of numerical simulation methods with thermal cycle-based microstructure prediction [12], but besides the high effort to gain accurate results, there is also a need for verification and calibration procedures.

In the event that mechanical properties with higher accuracy are needed, the only feasible method for the determination of the cooling time—mechanical property—relationship is the execution of welding experiments with subsequent destructive testing. This is of course not possible in productive environments without increasing effort and manufacturing costs of welded parts. It can be concluded that there is still no simple method available to estimate the mechanical properties of weld metals, based on measurements of welding process parameters or thermal properties.

Low-alloyed ferritic weld metals undergo solid state phase transformations during cooling, which can be detected through thermal analysis methods, such as dilatometry (DA), differential thermal analysis (DTA), or differential scanning calorimetry (DSC). The application of a DTA method in situ during welding provides the possibility to investigate phase transformations in consideration of the welding conditions. Solid state phase transformations in steels during cooling can be separated into two groups, reconstructive and displacive mechanisms [13]. The first group is characterized by diffusion-controlled nucleation and growth whereas the second group comprises shape deformations through diffusion (Widmanstätten ferrite) or diffusionless (martensite). Any change in cooling rate will therefore influence the phase transformation process, since nucleation and growth of the formed phase depend on the temperature. Besides, the amount of microstructure transformed at a given temperature determines if low temperature

transformations (e.g., bainitic and martensitic transformation) appear, since they contribute to a strength increase. Furthermore, the microstructural refinement caused by high cooling rates also influences the strength level. For a given chemical composition, the phase transformation temperature will be lowered when the cooling rate increases, since the diffusion processes, nucleation, and growth are all time dependent.

These evidences lead to the question if the strength of weld metals could be evaluated through monitoring of the phase transformation temperatures. In a preliminary study, the correlation between phase transformation temperature and ultimate tensile strength in all weld metal was investigated [14]. For multilayer, all weld metal samples of high-strength steels deposited using the gas metal arc welding process an almost linear regression function between tensile strength and transformation start temperature was found regardless of the steel composition. Since the alloying concept of welding filler wires differs significantly from rolled base metal plates, the influence of dilution on the transformation start temperature and the resulting mechanical properties when performing joint welding of HSLA steel plates were investigated here.

## 1.1 Experimental work

In this study, multilayer joint welds on a wide range of high-strength low-alloyed structural steel plates were prepared using a fully mechanized gas metal arc welding process in flat position. The considered base metals belonged to the group of high-strength low-alloyed structural steel heavy plates.

The high-strength steels used in this study were delivered in thermomechanical controlled processing state or quenched and tempered state. Additionally, a normalized fine-grained structural steel S355 N of a lower strength level was used for comparison (Tables 1 and 2).

The welding wires used were commercially available solid wires for high-strength low-alloyed steels according to the standard EN ISO 16834 [1]. As a reference, the very common welding wire grade G 3Si1 according to the standard EN ISO 14341 [15] was also tested. All welding wires had a diameter of 1.2 mm. The chemical compositions of multi-layer all-weld metal samples were determined using a spark optical emission spectrometer (Table 3). Three base metal yield strength levels of 960 MPa and above were considered within the investigation, in order to analyze the effect of dilution, when using the same welding filler wire G Mn4Ni2,5CrMo.

A commercially available welding power source Cloos Quinto GLC 503 was used in combination with a welding torch mounted in flat position on a linear table. The weld preparation was done by flame cutting with following superficial milling. In order to prevent weld deterioration and any influence on the weld geometry, the mill scale on both sides of the base plates was removed close to the welding zone by grinding. In a former study based on the same base materials, a strong impact of

**Table 1** Overview on the investigated steel grades and the corresponding filler metals

Steel type	Standard	Plate thickness [mm]	Processing	Yield strength [MPa]	Used filler metal
S355N	EN 10025-3 [16]	12	N	355	G 3Si1
S690QL	EN 10025-6 [17]	10	QT	690	G Mn3Ni1Mo
S960QL		12		960	G Mn4Ni2,5CrMo
S1100QL	–	11		1100	G Mn4Ni2,5CrMo
S700MC	EN 10149-2 [18]	12/40	TMCP	700	G Mn4Ni1,5CrMo
S960MC		12		960	G Mn4Ni2,5CrMo

**Table 2** Chemical composition of base metals (spark optical emission analysis)

Weight [%]	C	Mn	Si	Cr	Ni	Mo	Ti	Al	Nb	V
S355N	0.18	1.12	0.32	0.14	0.24	0.03	0.003	0.04	0.02	0.004
S690QL	0.15	1.18	0.26	0.33	0.04	0.21	0.003	0.08	0.03	0.008
S700MC (12 mm)	0.05	1.93	0.35	0.61	0.03	0.29	0.005	0.03	0.04	0.009
S700MC (40 mm)	0.04	1.62	0.35	0.41	0.02	0.23	0.013	0.03	0.04	0.045
S960MC	0.08	1.65	0.34	0.61	0.03	0.29	0.006	0.03	0.04	0.079
S960QL	0.14	1.14	0.25	0.59	0.36	0.32	0.005	0.07	0.03	0.054
S1100QL	0.11	0.94	0.23	0.61	1.96	0.60	0.003	0.04	0.02	0.005

residual mill scale on weld geometry and thermal cycle was found [19]. The base plates were clamped on the welding table through hydraulic clamps, which were released immediately after the final weld bead was placed, so that the residual stress level inside the weld could be minimized [20]. Load cells were used to monitor the clamping force during welding, but were not considered for later evaluation of residual stress since the setup was not optimized for this purpose (Fig. 1).

A single bevel butt joint geometry was used for all weldments (Fig. 2). The cooling curve of the weld metal was acquired during every weld run by a two-color pyrometer (Sensortherm Metis M3). The measuring spot of the pyrometer was set to the center surface of every weld bead. Since the physical quantity measured by a pyrometer is only indirectly linked to the surface temperature of the sample, it is inevitable to carry out a calibration procedure before starting the measurement. Therefore, base metal samples of all materials under investigation were heated using resistance heating blankets from room temperature up to 900 °C, whereas the temperature was kept constant in steps of 100 °C. The temperature was then measured using the pyrometer in quotient mode and a

thermocouple at the same time. The thermocouple had a diameter of 0.2 mm (Ni-/NiCr, type K). The acquisition was done using a National Instruments NI 9213 Thermocouple amplifier with internal cold junction compensation. It was found that the pyrometer quotient temperature reading for the considered measurement conditions differed up to 20 °C from the thermocouple measurement value. If weld metal temperature measurements are carried out during welding, additional influencing factors can deteriorate the accuracy of the measured values. Pyrometric measurements reflect the varying surface conditions due to the formation of an oxide scale layer and the thermal contraction. This leads to unstable transient signals. When using a two-color pyrometer, these factors are partially eliminated, but still depend strongly on the sample material and the process conditions.

For the experiments, three welding parameter sets were selected based on the usual heat input range applicable for the considered materials (Table 4). The electrical parameters were chosen in order to achieve a spray arc metal transfer, whereas the heat input was modified by changing the welding speed. Welding current and welding voltage were measured

**Table 3** Chemical composition of all weld metal samples

Weight [%]	C	Mn	Si	Cr	Ni	Mo	Ti	Al	Nb	V	Yield strength
G 3Si1	0.08	1.22	0.72	0.03	0.04	0.01	0.005	0.003	0.001	0.005	> 420
G Mn3Ni1Mo	0.08	1.39	0.57	0.08	0.92	0.39	0.031	0.004	0.001	0.006	> 640
G Mn4Ni1,5CrMo	0.08	1.34	0.54	0.27	1.69	0.52	0.022	0.004	–	0.005	> 880
G Mn4Ni2,5CrMo	0.11	1.65	0.66	0.43	2.32	0.50	0.023	0.004	0.001	0.007	> 930

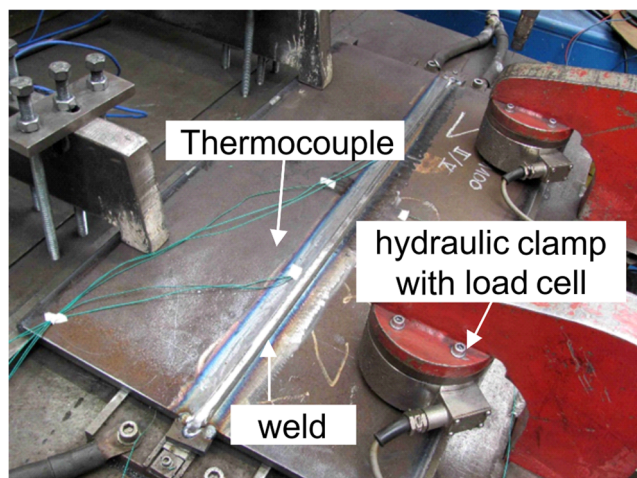


**Fig. 1** Welding setup with hydraulic clamping and thermocouple mounting position

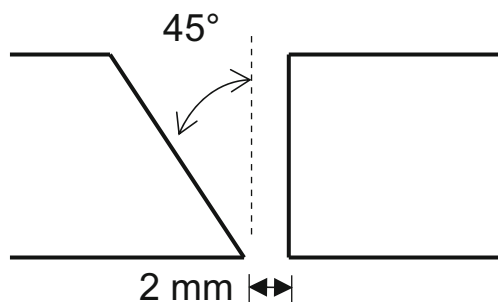


**Fig. 2** Single bevel butt weld preparation used for all weldments

with a sample rate of 1 kHz and the average values were determined by transient multiplication of current and voltage. All weldments were prepared by heating the plates prior to welding to a preheat temperature of 100 °C, measured at two locations according to EN ISO 13916 [21]. Every following up weld bead after the root weld was started at an interpass temperature of 150 °C, measured in the weld groove by a contact temperature sensor (type K Thermocouple).

After welding, a single longitudinal round tensile test specimen was machined from the upper region along the centerline of every weld (Fig. 3). All samples were prepared according to DIN 50125 [22] form B6x30 and were tested with a crosshead velocity of 1 mm/min following the procedure described in EN ISO 6892-1 (method A) [23]. Charpy-V notch impact test samples acc. to EN 148-1 [24] were machined out of the weld metal and the heat affected zone (three samples per weld). For

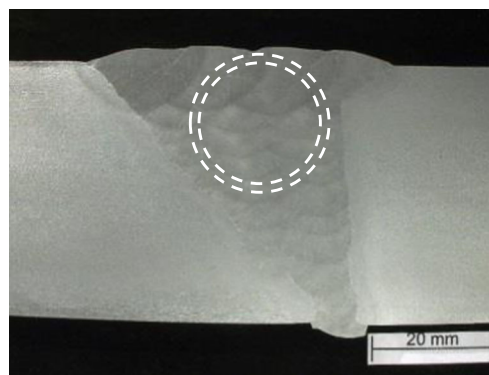


**Fig. 3** Sampling location for longitudinal round tensile test specimens

the evaluation of cooling times and transformation temperatures, the average value from the upper weld runs was considered wherein the tensile test sample was located. The determination of weld metal phase transformations through evaluation of the cooling curve was carried out in a comparable way to [25]. The qualification of this approach for the given weld metals has been described in [26]. The approach is based on the derivation of a fit function from the measured cooling curve in order to enable the determination of the transformation start temperature (Fig. 4). The microstructure of the weld metals were then examined under a light optical microscope after polishing and etching with Nital solution.

## 2 Results

The average cooling times between 800 and 500 °C of the top weld layers show a wide variation even for the same welding parameter set, when different base materials are compared (Fig. 5). Even though defined welding parameter sets were used in all experiments, a varying arc burning behavior was observed, which is common for welding filler wires and diluted base metals with varying chemical composition. This led to changed heat transfer into the weld pool. Furthermore, the weld bead geometry was not constant. Due to the design of the study, it was not important to have exactly matching cooling times in every experiment, since a correlation between input parameters and resulting mechanical properties is still visible when scattered values appear. Besides the influence of the cooling rate on the phase transformation temperature, the chemical composition was investigated (Fig. 6). Based on the formula proposed by Steven and Haynes [27], the bainite start

**Table 4** Welding parameters within the investigation

Heat input [kJ/cm]	Voltage [V]	Current [A]	Welding speed [cm/min]	Electrical power [kW]	Wire speed [m/min]	Deposition rate [kg/h]
16.2	27	280	28	7.6	8	4.3
11.6	27	280	39	7.6	8	4.3
7.0	27	280	65	7.6	8	4.3

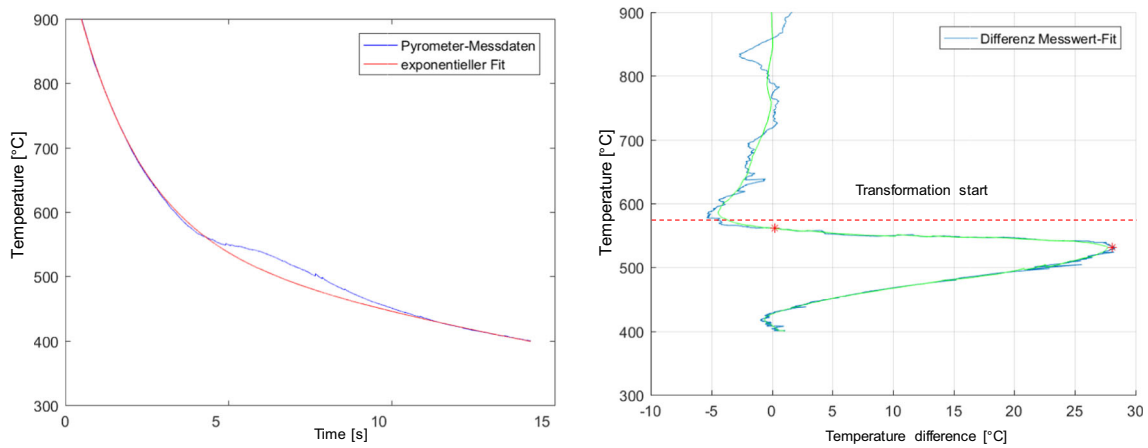


**Fig. 4** Example cooling curve with exponential fit (left), example temperature difference curve derived by subtraction of measured temperature from fit function (right) with marked transformation start temperature

**Fig. 5** Cooling time  $t_{8/5}$  and corresponding longitudinal ultimate tensile strength of high-strength weld metals in joint welds

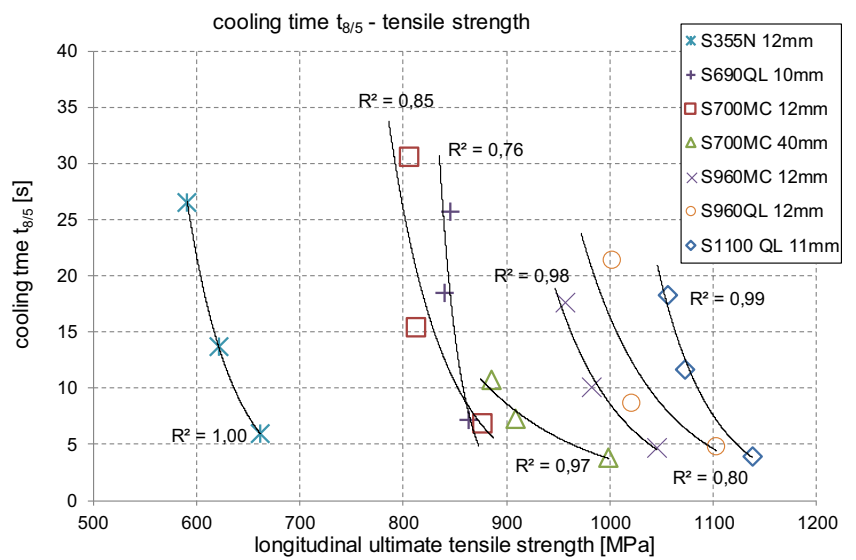


**Fig. 6** Transformation temperature over cooling time  $t_{8/5}$

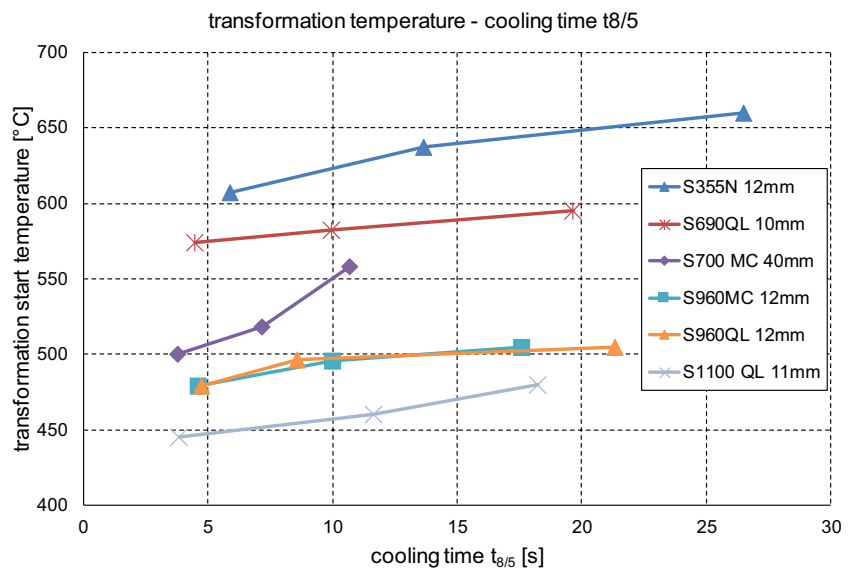
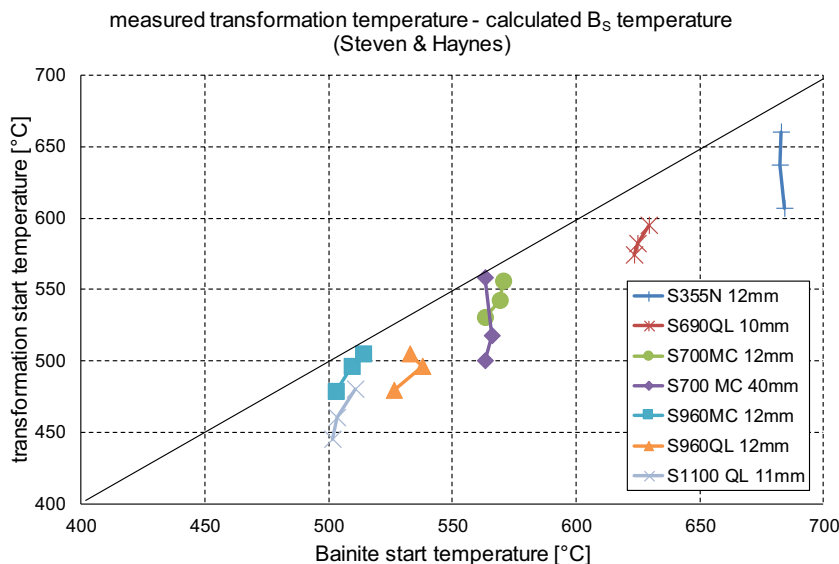




**Fig. 7** Measured phase transformation start temperature over calculated bainite start temperature after the formula proposed in [17]



temperature was then calculated for every sample. Only slight variations in the chemical composition lead to nearly constant calculated  $B_s$  temperatures whereas faster cooling leads to transformation retardation (Fig. 7). For every type of base material—filler metal combination a specific correlation between cooling time and longitudinal ultimate tensile strength can be found. Comparable correlations are found if other mechanical properties are considered, such as yield strength, fracture elongation, or notch impact toughness. A regression curve can be established through fitting of a power function.

In contrast to this, the consideration of the phase transformation start temperature below 800 °C and mechanical properties leads to a regression function, which is applicable for most considered weld metals, regardless of their strength level (coefficient of determination  $R^2 = 0.861$ ). For a given phase transformation temperature, the accuracy of the calculated longitudinal ultimate tensile strength varies between  $\pm 50$

and  $\pm 150$  MPa, depending on the strength level considered (Fig. 8). The empirical probability for the tensile strength to appear within the scatter band is 0.85. It is noteworthy that the weld metals of the S690QL and S1100QL welds deviate significantly from the regression curve. This is possibly induced by the differing alloying concept of both weld metals, which leads to higher ferrite content in S690QL weld metal and a certain martensite content in S1100QL weld metal. When regarding the transformation temperature dependence of the measured cooling time, the strong influence of chemical composition on the transformation temperature is visible (Fig. 6). Differences in the transformation temperature/cooling time behavior for the base metals S960MC/QL and S1100QL, which have been welded using the same type of filler wire (G Mn4Ni2.5CrMo), signify that the dilution of the base metal has to be taken into account. The variation in chemical composition for one welding parameter set is shown in Table 5. It

**Fig. 8** Transformation temperature over longitudinal ultimate tensile strength, dashed lines show fitted regression curve and the percentile  $P_{85}$

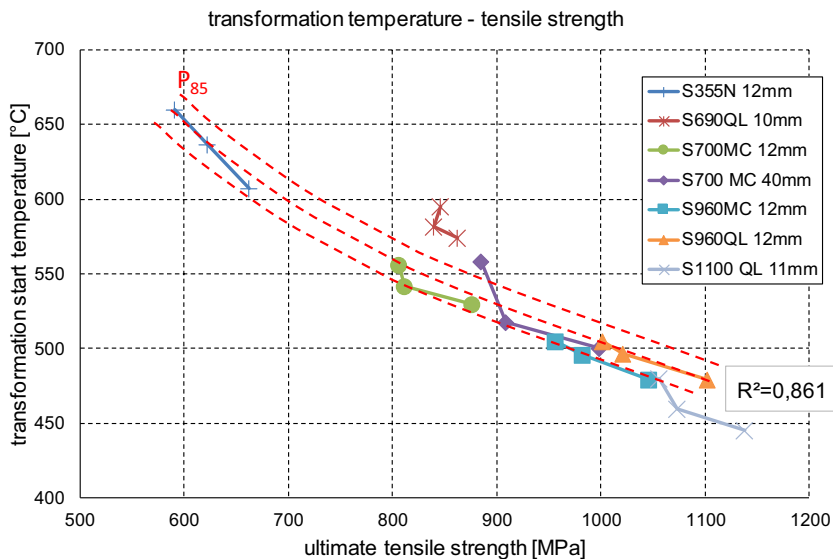


**Table 5** Weld metal chemical composition of selected samples, filler wire G Mn4Ni2,5CrMo,  $I=280$  A,  $U=27$  V, welding speed = 28 cm/min

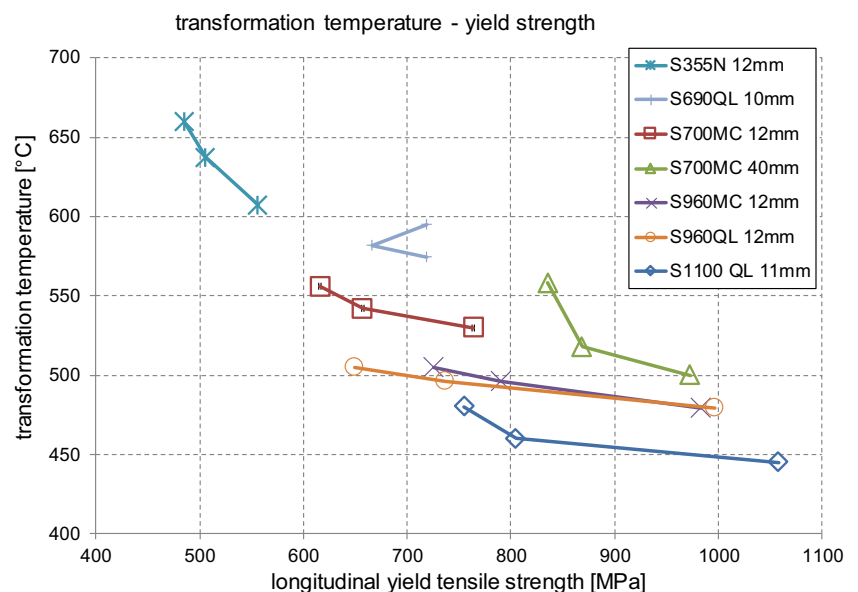
Weight [%]	C	Mn	Si	Cr	Ni	Mo	Ti	Al	Nb	V
S960MC	0.094	1.59	0.61	0.48	2.04	0.47	0.019	0.002	0.006	0.020
S960QL	0.118	1.46	0.54	0.45	1.80	0.43	0.017	0.009	0.005	0.017
S1100QL	0.124	1.35	0.50	0.52	2.24	0.55	0.022	0.011	0.009	0.007

is obvious that the transformation start temperature will be influenced therefore.

For the yield tensile strength curve, a comparable behavior can be observed (Fig. 9). All weld metals in which a filler wire of the type G Mn4Ni2,5CrMo was used show a very low significance level of the phase transformation temperature on the yield strength. This can be also observed when the fracture elongation is considered (Fig. 10). Notch impact toughness test at  $-40$  and  $-60$  °C showed that the phase transformation temperature can also be correlated with the resulting notch impact toughness (Figs. 11 and 12). The unsteady notch impact toughness values of some weldments (e.g., S355) were identified as related to partial covering of the base metal at the notch position.

Within the considered weld metal microstructures in a typical constitution for the respective chemical composition are found. For the C-Mn-Si-alloyed weld metal (S355 + G 3Si1) the microstructural constituents change from bainite and ferrite with secondary phases to acicular ferrite with polygonal grain boundary ferrite when the cooling time increases (Fig. 13a). For the weld metals with higher alloying element concentration, the amount of acicular ferrite (Fig. 13b) besides bainite increases. Even for the martensitic weld metal, the cooling time influences the microstructure with regard to the amount of tempered martensite.

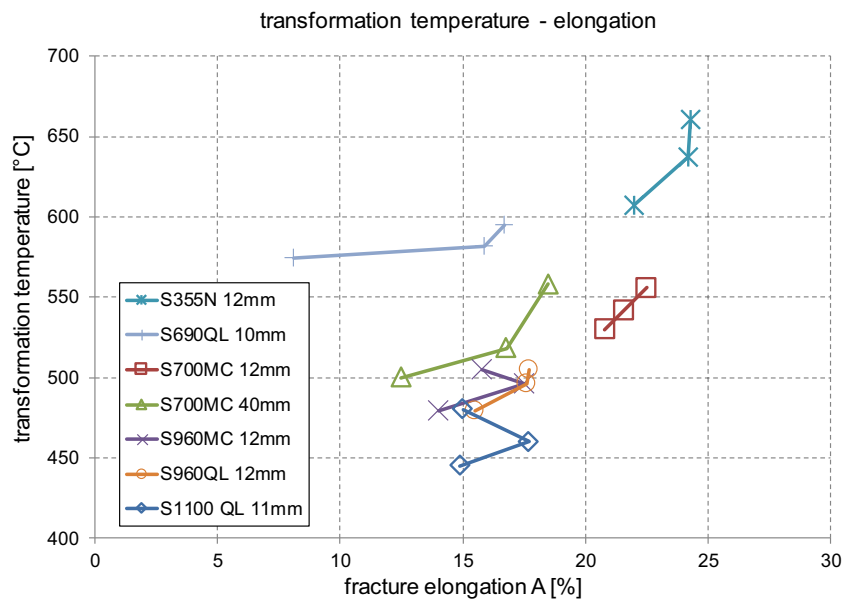
**Fig. 9** Transformation temperature and corresponding longitudinal yield tensile strength



### 3 Discussion

The presented results indicate a connection between solid state phase transformation temperatures and mechanical properties of weld metals in high-strength low-alloyed steels. Keeping in mind the basic information which can be gathered from CCT diagrams, this finding is nothing fundamentally new. However, using the correlation between phase transformation temperature and mechanical properties offers the advantage that without having materials' specific reference data, a rough estimation of properties is possible. A reason for some weld metals to show a higher deviation can be found when looking at the alloying element content (Tables 2 and 3). The weld metal of S690QL shows a higher transformation temperature than the S700MC weld metal, while the Nickel content in the latter is increased by 0.6% at the same time. For the weld metal of S1100QL with the highest strength level, the correlation accuracy is clearly reduced, due to the higher martensite content. Since the main influence on the transformation temperature are diffusion processes, a higher quantity of diffusionless microstructural transformations does influence the mechanical properties, but to a lower extent, the phase transformation temperature. This can be seen if the yield strength is considered (Fig. 9). Prior austenite grain size, oxygen, and nitrogen content are not analyzed here, but also

**Fig. 10** Transformation temperature and corresponding longitudinal fracture elongation



influence the ductility of weld metals. Given that the tendency stays the same (lower transformation start temperature leads to higher strength level), the scattering is elevated to a much higher extent. This is even more obvious for fracture elongation (Fig. 10).

Based on the presented results (Figs. 11 and 12) it is difficult to generally correlate the notch impact toughness to the phase transformation start temperature. Since the notch impact toughness is closely related to strength level,

microstructural constituent, and chemical composition, it is likely to assume that the visible influence on the toughness values is therefore indirectly promoted.

Due to the limited number of alloys considered within this study, the existence of other correlations was not investigated.

The presented method offers interesting possibilities for preliminary strength classification of mechanical properties in joint welds and all weld metals. This could support the alloy development process of filler metals for high-strength steels.

**Fig. 11** Transformation temperature and corresponding notch impact toughness at -40 °C

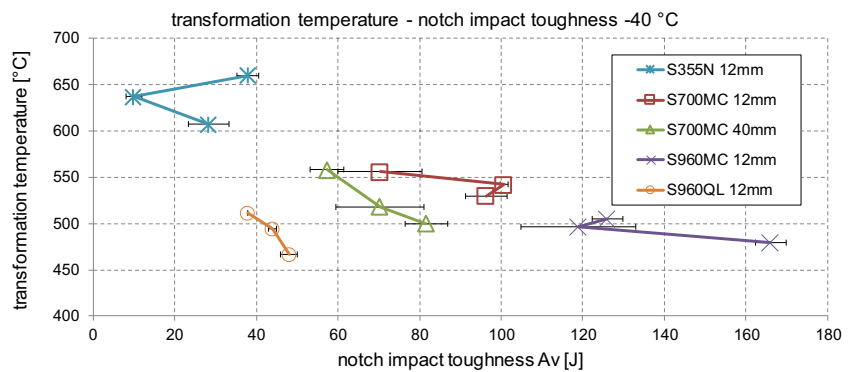


**Fig. 12** Transformation temperature and corresponding notch impact toughness at -60 °C

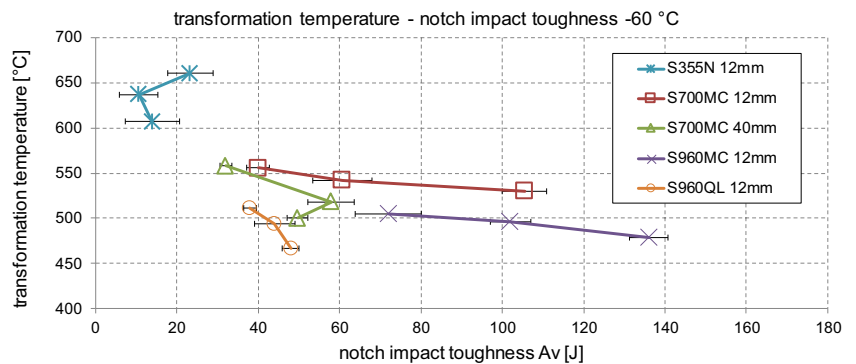
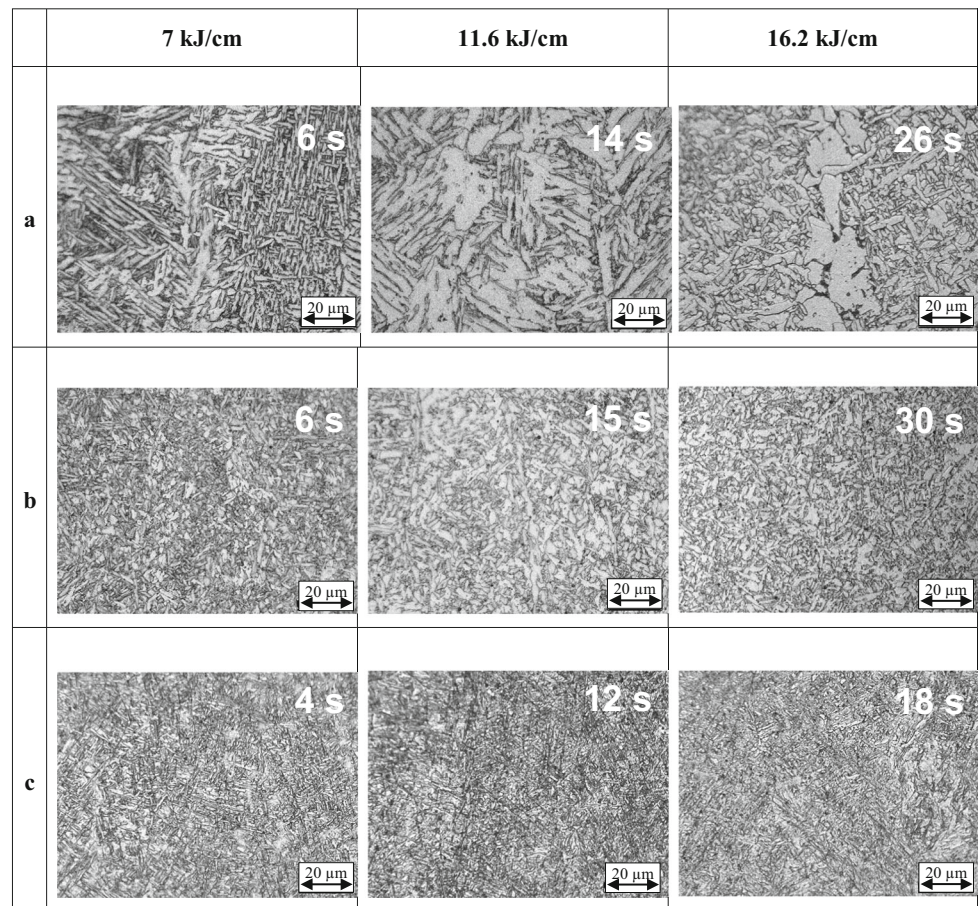




**Fig. 13** Micrographs of selected GMA weld metals (*a* = S355 N + G 3Si1, *b* = S700MC + G Mn4Ni1,5CrMo, *c* = S1100QL + G Mn4Ni2,5CrMo), cooling time  $t_{8/5}$



When compared to the common method for quality assurance based on the cooling time  $t_{8/5}$ , it is striking that the transformation temperature offers more diverse information about the alloy and resulting microstructure. A drawback is the higher complexity of measurement and the difficulties arising when the transformation temperature is to be calculated for a given weld metal under fixed welding conditions.

## 4 Conclusions

Based on the experimental work presented here, the following conclusions can be drawn:

1. The estimation of tensile strength based on a correlation to the cooling time  $t_{8/5}$  leads to applicable results, if the behavior of the specific material is known.
2. The phase transformation start temperature increases when the weld metal is subject to longer cooling times  $t_{8/5}$
3. A power function regression can be used to describe the ultimate tensile stress based on the measured transformation temperature
4. Lower accuracy will result when other mechanical properties are considered, such as yield strength, fracture elongation, or notch impact toughness.
5. For steel weld metals with mainly ferrite or martensite constituents, other correlations are possible

## 5 Summary

In this work, a method is presented to correlate the solid state phase transformation temperature of high-strength low-alloyed steel weld metals and mechanical properties after welding. Based on in-situ determination of the phase transformation temperature, tensile strength, yield strength, rupture elongation, and charpy notch impact toughness have been compared to investigate the dependency between these values. The investigated weld metals showed mainly bainitic transformations. Nevertheless, it is possible that martensitic transformations take place and lead to further correlation functions which should then be applied for weld metals with mostly martensitic phase transformations.

**Acknowledgements** All presented investigations were conducted in the context of the Collaborative Research Centre SFB1120 “Precision Melt Engineering” at RWTH Aachen University and funded by the German Research Foundation (DFG). For the sponsorship and the support, we wish to express our sincere gratitude.

## References

- EN ISO 16834:2012 Welding consumables—Wire electrodes, wires, rods and deposits for gas shielded arc welding of high strength steels—Classification
- AWS A5.28:2007 Specification for low-alloy steel electrodes and rods for gas shielded arc welding
- Grong Ø (1997) Metallurgical modelling of welding, 2nd edn. Institute of Materials, London, England
- Svensson LE, Grefott B, Bhadeshia HKDH (eds) (1986) An analysis of cooling curves from the fusion zone of steel weld deposits. *Scand J Metall* 15:97–103
- Kas, J., van Adrichem, T. J. (1969) Einfluss der Schweißparameter auf den Abkühlverlauf in der Schweißverbindung, Schweißen und Schneiden 21,5, 199–203
- Uwer D, Degenkolbe J (1975) Temperaturzyklus beim Lichtbogenschweißen—Einfluss des Wärmebehandlungszustandes und der chemischen Zusammensetzung von Stählen auf die Abkühlzeit. *Schweißen und Schneiden* 27(8):303–306
- Lalam SH, Bhadeshia HKDH, MacKay DJC (2000) Estimation of mechanical properties of ferritic steel welds. Part 1: yield and tensile strength. *Sci Tech Weld Join* 5(3):135–147. <https://doi.org/10.1179/136217100101538137>
- Lalam SH, Bhadeshia HKDH, MacKay DJC (2000) Estimation of the mechanical properties of ferritic steel welds: part II: elongation and charpy toughness. *Sci Tech Weld Join* 2000(5):149–160. <https://doi.org/10.1179/136217100101538146>
- Ilman MN, Cochrane RC, Evans GM (2012) Effect of nitrogen and boron on the development of acicular ferrite in reheated C-Mn-Ti steel weld metals. *Weld World* 56:41–50. <https://doi.org/10.1007/BF03321394>
- Ilman MN, Cochrane RC, Evans GM (2014) Effect of titanium and nitrogen on the transformation characteristics of acicular ferrite in reheated C-Mn steel weld metals. *Weld World* 58:1–10. <https://doi.org/10.1007/s40194-013-0091-x>
- Keehan E, Zachrisson J, Karlsson L (2010) Influence of cooling rate on microstructure and properties of high strength steel weld metal. *Sci Tech Weld Join* 15(3):233–238. <https://doi.org/10.1179/136217110X12665048207692>
- Toyoda M, Mochizuki M (2003) Control of mechanical properties in structural steel welds by numerical simulation of coupling among temperature, microstructure, and macro-mechanics. *Sci Tech Adv Mat* 5(1–2):255–266. <https://doi.org/10.1016/j.stam.2003.10.027>
- Bhadeshia, H. K. D. H. (1998) ‘Modelling of phase transformations in steel welds’ proceedings of ECOMAP ‘98 Kyoto, Japan, published by the High Temperature Society of Japan, 1998, 35–44
- Sharma R, Reisgen U (2016) ‘Cooling curve based estimation of mechanical properties in high strength steel welds’, Proceedings of Thermec 2016, Graz. *Mat Sci Forum* 879:1760–1765. <https://doi.org/10.4028/www.scientific.net/MSF.879.1760>
- EN ISO 14341:2011 Welding consumables—Wire electrodes and weld deposits for gas shielded metal arc welding of non-alloy and fine grain steels—Classification
- EN 10025-3:2011 Hot rolled products of structural steels—Part 3: Technical delivery conditions for normalized/normalized rolled weldable fine grain structural steels;
- EN 10025-6:2011 Hot rolled products of structural steels—Part 6: technical delivery conditions for flat products of high yield strength structural steels in the quenched and tempered conditions
- EN 10149-2:2013 Hot rolled flat products made of high yield strength steels for cold forming—Part 2: technical delivery conditions for thermomechanically rolled steels
- Sharma, R, Reisgen, U. (2016) ‘Influence of mill scale on weld bead geometry and thermal cycle during GTA welding of HSLA steels’, IIW Doc. IX-L-1155-16, 69th Annual Assembly of IIW, Melbourne, Australia
- Schröpfer D, Kannengiesser T, Kromm A (2014) Influence of heat control on welding stresses in multilayer-component welds of high-strength steel S960QL. *Adv Mater Res* 996:475–480. <https://doi.org/10.4028/www.scientific.net/AMR.996.475>
- EN ISO 13916:2017 Welding—Measurement of preheating temperature, interpass temperature and preheat maintenance temperature
- DIN 50125:2016 Testing of metallic materials—Tensile test pieces
- EN ISO 6892-1:2016 Metallic materials—Tensile testing—Part 1: method of test at room temperature
- EN ISO 148-1:2016 Metallic materials—Charpy pendulum impact test—Part 1: test method
- Alexandrov, B.T., Lippold, J.C. (2004) ‘Methodology for in situ investigation of phase transformations in welded joints’, IIW. Doc. IX-2114-04, 57th Annual Assembly of IIW, Osaka, Japan
- Sharma R, Reisgen U (2017) Comparative study of phase transformation temperatures in high strength steel weld metals. *Materials Testing* 59(4):344–347. <https://doi.org/10.3139/120.111003>
- Steven W, Haynes AG (1956) The temperature of formation of martensite and bainite in low-alloy steel. *J Iron Steel Inst* 8:349–359